the maximum point in the intensity spectrum by f_{max} and the corresponding phase angle by ϕ_{max}, the phase difference at the maximum point is $2n\pi$, which yields

$$2\pi f_{max} \times \frac{2d}{c_0} = \phi_{max} + 2n\pi \tag{3}$$

The phase angles ϕ_{min} and ϕ_{max} can be expressed by

$$2\pi f_{min} \times 2d\left(\frac{1}{c_0} - \frac{1}{c}\right) = \phi_{min} \tag{4}$$

$$2\pi f_{max} \times 2d\left(\frac{1}{c_0} - \frac{1}{c}\right) = \phi_{max} \tag{5}$$

since ϕ_{min} or ϕ_{max} is the phase difference between the wave that travels the distance $2d$ with sound speed c and the wave that travels a corresponding distance with sound speed c_0. By solving Eqs. (2) and (4),

$$d = \frac{c_0}{4\pi f_{min}}\{\phi_{min} + (2n-1)\pi\} \tag{6}$$

is obtained for the minimum point. Solving Eqs. (3) and (5) yields

$$d = \frac{c_0}{4\pi f_{max}}(\phi_{max} + 2n\pi) \tag{7}$$

for the maximum point. Finally, the sound velocity at each frequency is calculated as

$$c = \left(\frac{1}{c_0} - \frac{\phi_{min}}{4\pi f_{min} d}\right) \tag{8}$$

$$c = \left(\frac{1}{c_0} - \frac{\phi_{max}}{4\pi f_{max} d}\right) \tag{9}$$

After determination of the thickness, attenuation of ultrasound was then calculated by dividing amplitude by the thickness.

3. Results

Fig. 4 shows a PC window of our ultrasonic speed microscopy. The upper left is an amplitude image, the upper right is an ultrasonic speed image, the lower left is an attenuation image and the lower right is the thickness distribution of the normal coronary artery. The intima is thin and speed of sound is 1600 m/s in the intima, 1560 m/s in the media and 1590 m/s in the adventitia, respectively. Fig. 5 is an atherosclerotic coronary artery. The speed of sound is 1680 m/s in the thickened intima with collagen fiber, 1520 m/s in lipid deposition underlying fibrous cap and 1810 m/s in calcified lesion in the intima.

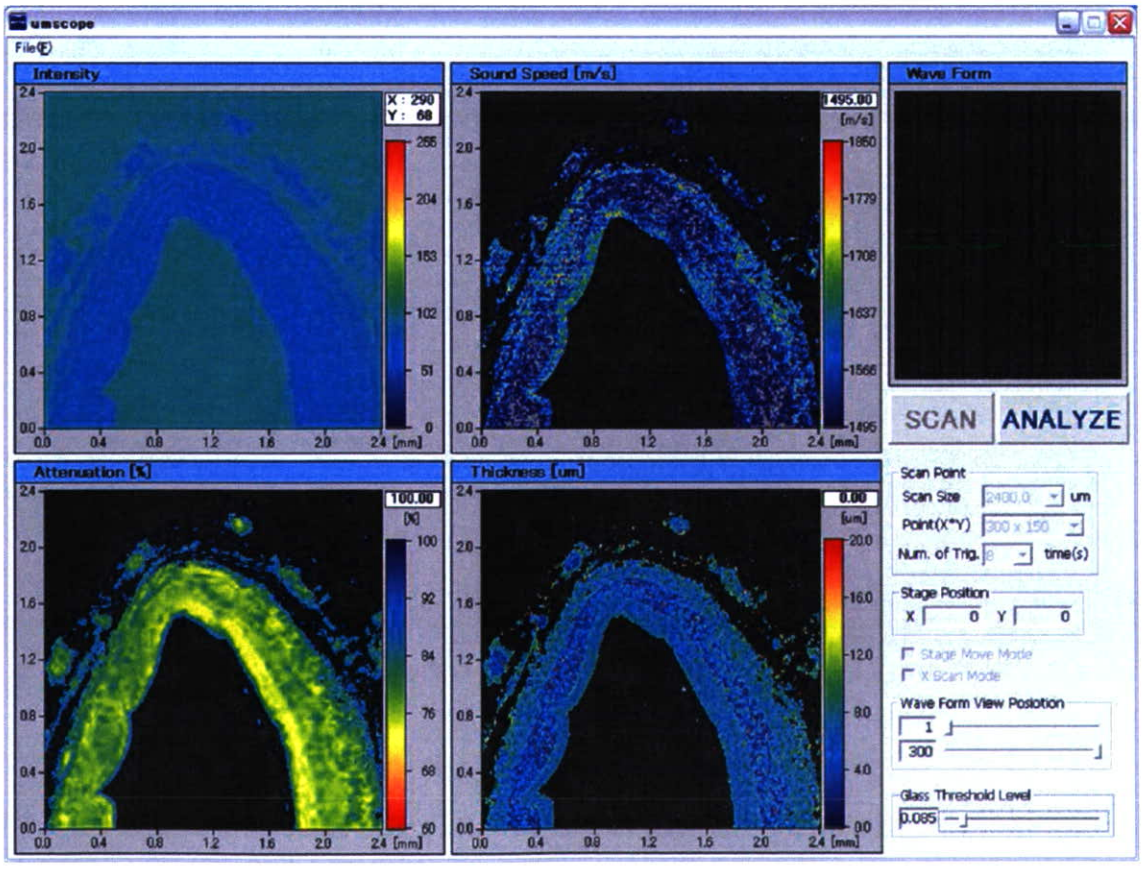

Fig. 4. PC window of ultrasonic speed microscopy showing a normal coronary artery. Upper left: amplitude image, upper right: speed of sound image, lower left: attenuation image and lower right: thickness.

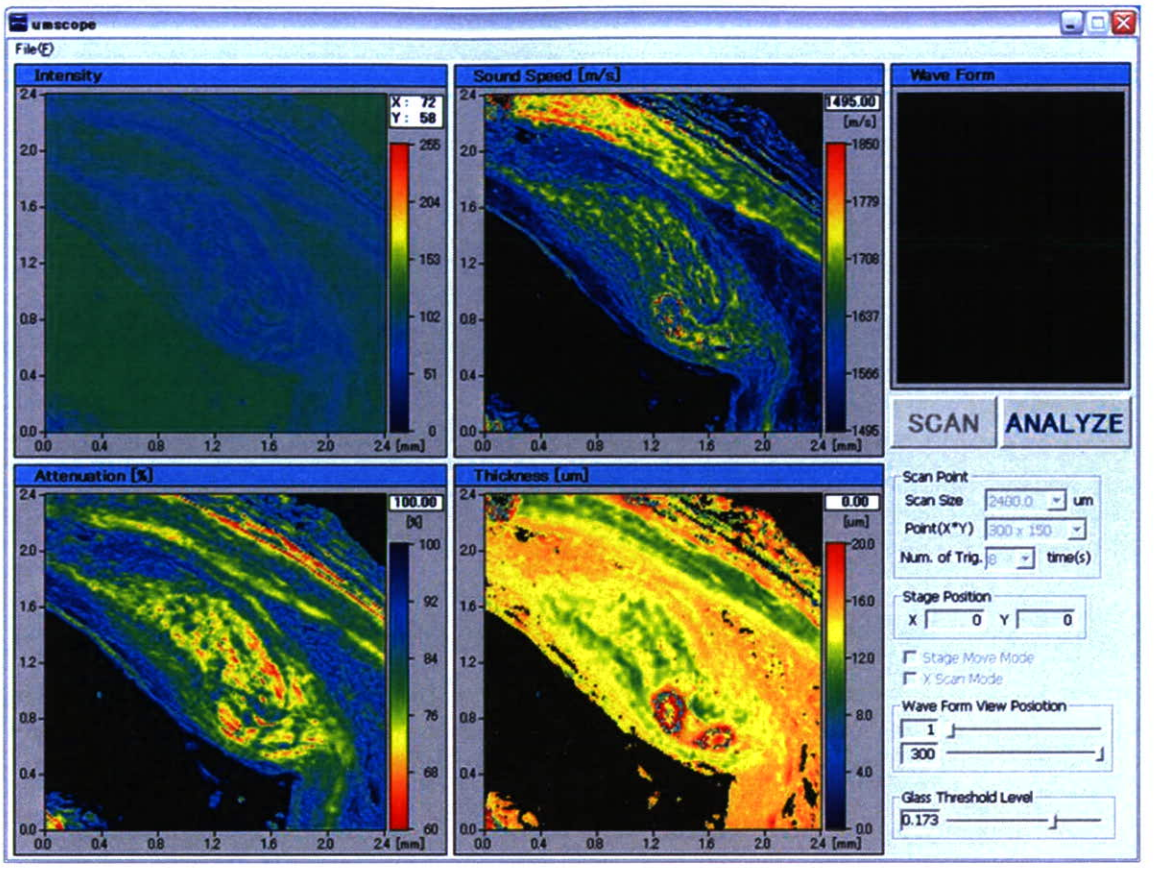

Fig. 5. PC window of ultrasonic speed microscopy showing an atherosclerotic coronary artery. Upper left: amplitude image, upper right: speed of sound image, lower left: attenuation image and lower right: thickness.

4. Discussion

In the present study, speed of sound in the excised human coronary arteries was measured with the ultrasonic speed microscopy. The results would become basic data base for interpretation of clinical IVUS images and novel IVUS imaging technologies.

The results showed that the speed of sound in the intima and adventitia, mainly consisted of collagen fiber, had higher values than those of media, mainly consisted of vascular smooth muscle. The different of acoustic properties may lead to the classical three-layered appearance of normal coronary artery in clinical IVUS imaging. The findings indicate that the echo intensity is not determined by the difference of acoustic impedance between neighboring layers. The distribution and the structure of materials with different acoustic properties may also contribute to the echo pattern in IVUS.

The plaque with a thick fibrous cap consisted of collagen fiber, considered showed higher value of speed of sound than those of normal media. Generally, absorption and scattering are the two main factors of attenuation of ultrasound. Thus, the high scattering within the thickened intima may lead to the high intensity echo in the "hard plaque". Lipid showed speed of sound. These values explain the low echo in the "soft plaque" in the same manner of renal cysts containing water like fluid. Besides its absolute low values, the homogeneity of acoustic properties within the lipid pool may contribute to the low scattering and consequently a lipid pool shows low intensity echo.

5. Conclusions

We have developed a novel acoustic microscope system that can measure the speed of sound of thin slices of biological material. The most important feature was use of a single pulse and the Fourier transform to calculate the sound speed at all measuring points. Although the data acquisition time of a frame was greater than that in conventional SAM, the total time required for calculation was significantly shorter. The acoustic microscope system can be applied to intraoperative pathological examination.

Acknowledgements

This study was supported by Grants-in-Aid for Scientific Research (Scientific Research (B) 15300178, Scientific Research (B) 15360217) from the Japan Society for the Promotion of Science and Health and Labor Sciences Research Grants from the Ministry of Health, Labor and Welfare for the Research on Advanced Medical Technology (H17-Nano-001).

References

[1] Y. Saijo, M. Tanaka, H. Okawai, F. Dunn, The ultrasonic properties of gastric cancer tissues obtained with a scanning acoustic microscope system, Ultrasound Med. Biol. 17 (1991) 709–714.
[2] H. Sasaki, M. Tanaka, Y. Saijo, H. Okawai, Y. Terasawa, S. Nitta, K. Suzuki, Ultrasonic tissue characterization of renal cell carcinoma tissue, Nephron 74 (1996) 125–130.
[3] Y. Saijo, M. Tanaka, H. Okawai, H. Sasaki, S. Nitta, F. Dunn, Ultrasonic tissue characterization of infarcted myocardium by scanning acoustic microscopy, Ultrasound Med. Biol. 23 (1997) 77–85.
[4] Y. Saijo, H. Sasaki, H. Okawai, S. Nitta, M. Tanaka, Acoustic properties of atherosclerosis of human aorta obtained with high-frequency ultrasound, Ultrasound Med. Biol. 24 (1998) 1061–1064.
[5] Y. Saijo, H. Sasaki, M. Sato, S. Nitta, M. Tanaka, Visualization of human umbilical vein endothelial cells by acoustic microscopy, Ultrasonics 38 (2000) 396–399.
[6] Y. Saijo, T. Ohashi, H. Sasaki, M. Sato, C.S. Jorgensen, S. Nitta, Application of scanning acoustic microscopy for assessing stress distribution in atherosclerotic plaque, Ann. Biomed. Eng. 29 (2001) 1048–1053.
[7] H. Sasaki, Y. Saijo, M. Tanaka, S. Nitta, Influence of tissue preparation on the acoustic properties of tissue sections at high frequencies, Ultrasound Med. Biol. 29 (2003) 1367–1372.
[8] Y. Saijo, T. Miyakawa, H. Sasaki, M. Tanaka, S. Nitta, Acoustic properties of aortic aneurysm obtained with scanning acoustic microscopy, Ultrasonics 42 (2004) 695–698.
[9] H. Sano, Y. Saijo, S. Kokubun, Material properties of the supraspinatus tendon at its insertion – A measurement with the scanning acoustic microscopy, J. Musculoskeletal Res. 8 (2004) 29–34.
[10] N. Hozumi, R. Yamashita, C.K. Lee, M. Nagao, K. Kobayashi, Y. Saijo, M. Tanaka, N. Tanaka, S. Ohtsuki, Time–frequency analysis for pulse driven ultrasonic microscopy for biological tissue characterization, Ultrasonics 42 (2004) 717–722.

Available online at www.sciencedirect.com
ScienceDirect
Ultrasonics 44 (2006) e147–e151
Ultrasonics
www.elsevier.com/locate/ultras

Intravascular two-dimensional tissue strain imaging

Yoshifumi Saijo [a,*], Akira Tanaka [b], Takahiro Iwamoto [c], Esmeraldo dos Santos Filho [c], Makoto Yoshizawa [c], Akira Hirosaka [d], Mikihiro Kijima [e], Yoshihisa Akino [f], Yasushi Hanadate [f], Tomoyuki Yambe [a]

[a] *Department of Medical Engineering and Cardiology, Institute of Development, Aging and Cancer, Tohoku University, 4-1 Seiryomachi, Aoba-ku, Sendai 980-8575, Japan*
[b] *Faculty of Symbiotic Systems Science, Fukushima University, Japan*
[c] *Information Synergy Center, Tohoku University, Japan*
[d] *Department of Cardiology, Ohta Nishinouchi General Hospital, Japan*
[e] *Department of Cardiology, Hoshi General Hospital, Japan*
[f] *Department of Cardiology, Miyagi Social Insurance Hospital, Japan*

Available online 5 July 2006

Abstract

Our goal is to achieve the precise quantitative imaging of tissue elasticity in clinical settings. In the present study, we measured basic ultrasonic characteristics of atherosclerosis by two-dimensional (2D) intravascular tissue velocity imaging.

Radio-frequency (RF) signal from a clinically used IVUS apparatus was digitized at 500 MSa/s and stored in a workstation. First, the correlation coefficient between two consecutive frames was calculated in the rotational direction and the rotational disuniformity was corrected to obtain the maximum correlation coefficient. Then, the polar coordinate images were converted into rectangular coordinate images and the images were divided into 64 by 64 square shaped regions of interest (ROIs). The correlation and displacement of the ROIs between the consecutive two frames were calculated by template matching method. Two-dimensional tissue velocity was defined as the vectors of displacement of ROI with 0.7 and more correlation.

IVUS studies were performed in directional coronary atherectomy (DCA) procedures. The specimens excised by DCA were stained with Elastica-Masson's trichrome staining and CD68 immunochemical staining.

Eleven cases (including two no re-flow cases and one perforation case) were intraoperatively observed by IVUS and the specimens obtained by DCA were observed by optical microscopy. The specimen from homogeneous 2D strain was collagen dominant fibrosis and the specimen from a lesion with complex vectors contained CD68 positive cells and degenerated collagen fibers, which indicated the plaque was vulnerable.

Keywords: Intravascular ultrasound; Tissue velocity imaging; Strain; Coronary artery; Atherosclerosis

1. Introduction

Intravascular ultrasound (IVUS) has been clinically applied since early 1990s and it has become an important clinical tool for investigation of coronary artery during percutaneous transluminal coronary intervention (PCI) therapies. IVUS is mainly used to measure the luminal and vascular areas and to confirm the full expansion of the coronary stent to the arterial wall. Besides the measurement of dimensions, IVUS also provides important information on tissue character of atherosclerosis. As the coronary artery is always receiving the blood flow and blood pressure, the dynamic characteristics of coronary artery are also examined. Erasmus University group lead by van der Steen has developed vascular "elastography"

* Corresponding author. Tel.: +81 22 717 8514; fax: +81 22 717 8518.
E-mail address: saijo@idac.tohoku.ac.jp (Y. Saijo).

0041-624X/$ - see front matter © 2006 Elsevier B.V. All rights reserved.
doi:10.1016/j.ultras.2006.06.049

technique using phased array IVUS of 20 MHz ultrasound [1–3].

However, mechanically rotating IVUS systems with the frequency between 35–40 MHz are mainly used in clinical cardiology because the image quality is better than that of phased array IVUS with the frequency of 20 MHz. One of the main objectives of the present study is to develop a quantitative method to assess tissue characteristics of coronary artery by analyzing radio-frequency (RF) signal from a mechanically rotating IVUS system. Especially, two-dimensional tissue velocity vector and strain of coronary artery are obtained and displayed on a conventional IVUS image.

In the present study, ultrasonic properties of atherosclerotic specimens excised by directional coronary atherectomy (DCA) are observed *in vivo* by IVUS tissue velocity imaging and are measured *in vitro* by optical microscopy.

2. Methods

2.1. Two-dimensional coronary tissue strain imaging

A commercial available IVUS system (Clear View Ultra, Boston Scientific, USA) was equipped. The central frequency of the IVUS probe (Atlantis SR Pro, Boston Scientific, USA) was 40 MHz and the pulse repetition rate was 7680 Hz. A single frame of the IVUS system consisted of 256 lines so that 7680 pulses made 30 frames per second (f/s). An analogue to digital (A/D) converter board (CompuScope 8500, Gage, USA) was connected to the RF (radio-frequency signal) output of the IVUS apparatus. The sampling rate was 500 megasamples per second (MSa/s), the resolution was 8-bit and the on-board memory was 8 MB. Intracoronary pressure was measured by fluid-filled method using 6 French (2.0 mm) diameter guiding catheter which was inserted into coronary artery.

Biological signals such as electrocardiogram and intracoronary pressure were simultaneously recorded using an A/D converter (PCI-6024E, National Instruments, USA) with the sampling rate of 100 kSa/s and the resolution of 12-bit. After the RF data were sent to the workstation, the signals were pre-treated for tissue velocity analysis. First, 30–50 MHz components of the original RF signal were extracted by using a software-based bandpass filtering method. Second, the original signal consisting of one line was divided into 10 matrixes. Each matrix consisted of 3053 lines by 256 columns and processed for one frame of IVUS image.

Ideally, one frame consisting of 256 lines of the rotational IVUS is equivalent to that of phased array IVUS. However, a conventional rotating IVUS system uses frame trigger to adjust frame to frame rotational non-uniformity. This indicates the position of the 'n/256'th line is not guaranteed to be at the same position of the previous frame. Then the correlation coefficient between two consecutive matrixes was calculated in the rotational direction and the rotational disuniformity was corrected in rotational direction to obtain the maximum correlation coefficient.

Conventional IVUS image was generated by converting polar coordinate of original RF signal matrix to rectangular coordinate. Then the IVUS image was divided into 64 by 64 square shaped regions of interest (ROIs). Template matching method was applied for calculation of correlation and displacement of the ROIs between the consecutive two frames. Template matching is the process of determining the presence and the location of a reference image or an object inside a scene image under analysis by a spatial cross-correlation process. Fig. 1 shows the schematic illustration of template matching method. If the coordinates of the center of the ROI in the first frame (a) is defined as $\boldsymbol{p}$ (0, 0) and the most similar patterned ROI in the next frame (b) is $\boldsymbol{q}$ (k, l), the correlation is given by Eq. (1).

$$R_{fg}(k,l) = \frac{\sum_{i=0}^{n^2-1}(f_i - \bar{f}_i)(g_i - \bar{g}_i)}{\sqrt{\sum_{i=0}^{n^2-1}(f_i - \bar{f}_i)^2 \sum_{i=0}^{n^2-1}(g_i - \bar{g}_i)^2}} \cdots \quad (1)$$

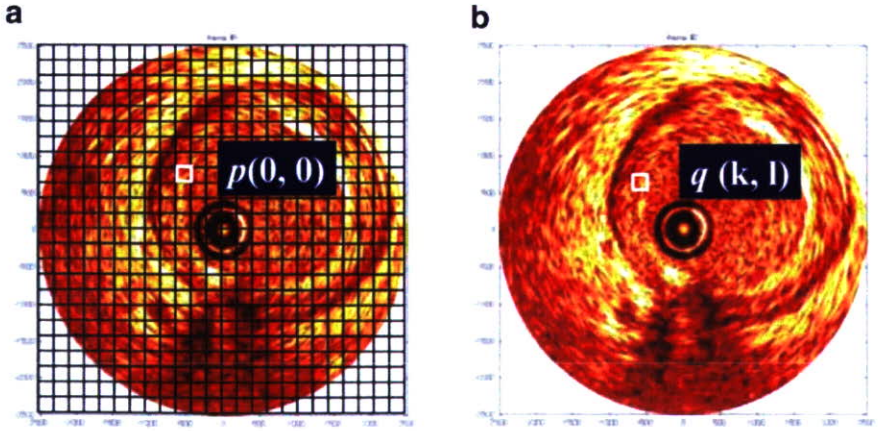

Fig. 1. Schematic illustration of template matching method. The coordinates of the center of the ROI in the first frame (a) is defined as $\boldsymbol{p}$ (0, 0) and the most similar patterned ROI in the next frame (b) is $\boldsymbol{q}$ (k, l).

Two-dimensional tissue velocity was defined as Eq. (2).

$$V = \arg\max_{k,l} R_{fg}(k,l) \cdots \quad (2)$$

Practically, the ROIs with low correlation should be considered as very fast moving targets such as blood flow or surrounding tissue. The vessel wall is considered stable during 1/30 s and we assume that the ROIs with high correlation coefficient correspond with vessel wall. Then 2D tissue velocity is displayed on the ROI with 0.7 and more correlation coefficient. Finally, the velocity is overlaid on a conventional IVUS image.

Tissue strain was defined as the deformation of the ROI area between two frames. Fig. 2 shows an example. If the four ROIs move to the same direction in Fig. 2(a), the area of the square (with solid lines) after deformation drawn by connecting center of ROIs is not changed from the original square (with dotted lines). But in case the four ROIs move to the different direction in Fig. 2(b), the area of the square (with solid lines) after deformation is expanded from the original square (with dotted lines). According to the color scale expressing area change, 2D tissue strain imaging is overlaid on the conventional IVUS image. Similar to the case of 2D tissue velocity imaging, color scale is only represented on the ROIs with higher correlation coefficient.

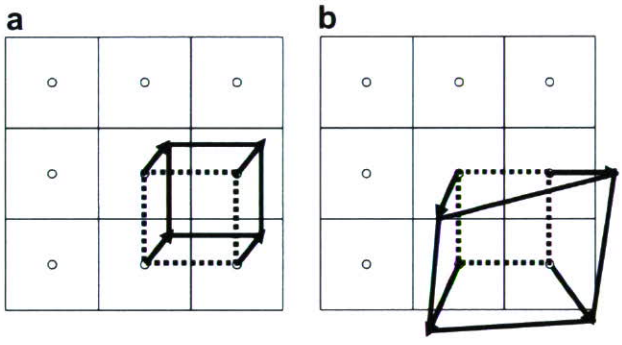

Fig. 2. Schematic illustration showing how to obtain 2D tissue strain imaging from 2D tissue velocity data.

2.2. Clinical data sampling

IVUS studies were performed in directional coronary atherectomy (DCA) procedures. The specimens excised by DCA were stained with Elastica-Masson's trichrome staining and CD68 immunochemical staining.

Eleven cases (including two no re-flow cases and one perforation case) with written informed consent were involved in the present study. Before DCA procedure, routine IVUS observation was performed and RF signal was acquired at the same moment. The excised samples were fixed by 10% formalin and stained with normal Elastica-Masson's trichrome staining and CD68 monoclonal staining.

3. Results

Fig. 3 shows (a) Color-coded IVUS, (b) two-dimensional correlation, (c) intracoronary blood pressure and timing of

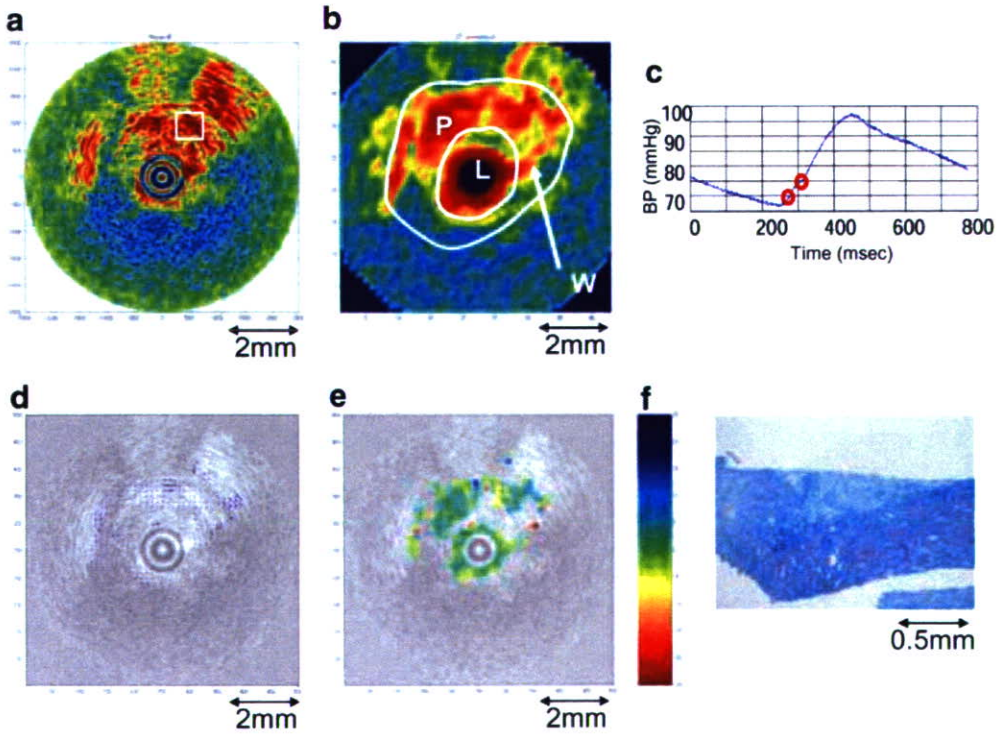

Fig. 3. (a) Color-coded IVUS, (b) two-dimensional correlation, (c) intracoronary blood pressure and timing of the two consecutive frames used in the analysis, (d) two-dimensional tissue velocity vector, (e) two-dimensional tissue strain and (f) optical microscope image of the excised specimen, of a homogeneous plaque. The square in Fig. 3(a) indicates where the sample was excised. L: lumen, P: plaque, W: vessel wall.

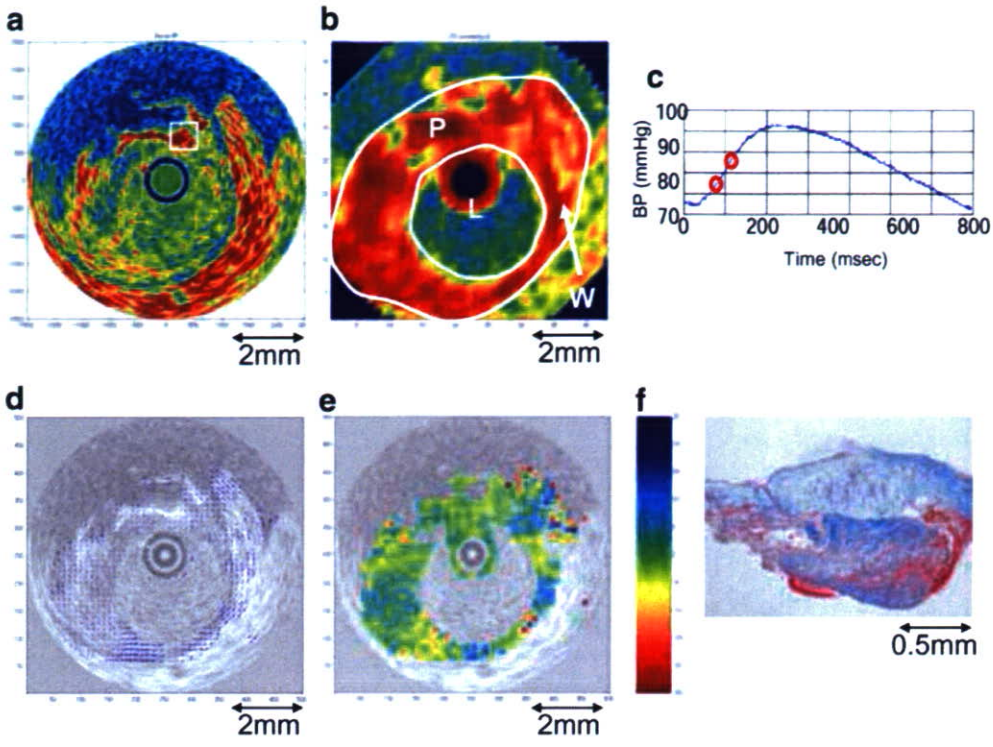

Fig. 4. (a) Color-coded IVUS, (b) two-dimensional correlation, (c) intracoronary blood pressure and timing of the two consecutive frames used in the analysis, (d) two-dimensional tissue velocity vector, (e) two-dimensional tissue strain and (f) optical microscope image of the excised specimen, of a inhomogeneous plaque. The square in Fig. 3(a) indicates where the sample was excised. L: lumen, P: plaque, W: vessel wall.

the two consecutive frames used in the analysis, (d) two-dimensional tissue velocity vector, (e) two-dimensional tissue strain and (f) optical microscope image of the excised specimen, of a homogeneous plaque. The square in Fig. 3 (a) indicates where the sample was excised. Color-coded IVUS image shows high intensity echo in the lesion. Two-dimensional correlation image shows the luminal border clearly. Two-dimensional tissue velocity vectors are almost same direction. Two-dimensional tissue strain shows the homogeneous strain pattern. The specimen is collagen rich fibrosis without macrophage infiltration. Fig. 4 shows (a) color-coded IVUS, (b) two-dimensional correlation, (c) intracoronary blood pressure and timing of the two consecutive frames used in the analysis, (d) two-dimensional tissue velocity vector, (e) two-dimensional tissue strain and (f) optical microscope image of the excised specimen of a heterogeneous plaque. The square in Fig. 4(b) indicates where the sample was excised. Two-dimensional tissue velocity and strain show heterogeneous patterns. The optical microscope image of the excised specimen showed various tissue components including hemorrhage. CD68 imaging showed infiltration of macrophages in this sample.

4. Discussion

The term "Elastography" was originally proposed by Ophir at University of Texas [4].

The method is based on external tissue compression, with subsequent computation of the strain profile along the transducer axis, which is derived from cross-correlation analysis of pre- and post-compression A-line pairs. Thus the precision of the positioning of RF-line pair is very important for the analysis.

The group at Erasmus University lead by van der Steen and de Korte has been applying the technique for vascular tissues. They have been using phased array IVUS system because RF-line pairs between pre and post frames are always guaranteed as coming from the same position of the tissue. Correlation analysis between two consecutive frames using rotating IVUS has been considered as difficult and has not been used for elastography. However, rotating-type IVUS is mainly used clinically because the catheter size is smaller and image quality is better than those with phased array IVUS because of the higher ultrasonic frequency. Especially, the identification of the coronary neo-intima at the follow up study is important in clinical situation and the rotating IVUS is superior in detecting neo-intima.

In the present study, the correlation image clearly identified the vascular wall of coronary artery. In the luminal area, correlation coefficient was low because blood was moving from observed plane to non-observed plane in the next frame.

The tissue receives blood pressure and shear stress caused by blood flow during cardiac cycles. Especially, the effect of blood pressure in the radial direction is important in determining 2D tissue velocity. The displacement caused by blood pressure would be large in the soft material and the displacement would be small in the hard material. Regarding 2D

tissue strain in our method, the physical meaning is not simple. If the material is homogeneous, the material would receive same load and deform uniformly. The local deformation would be random in the inhomogeneous material.

The two-dimensional tissue velocity and strain derived by the present method provide important information on tissue character. Stable plaque with dominant collagen fibrosis showed homogeneous strain. In contrast, a vulnerable plaque showed heterogeneous strain indicating the tissue components are also inhomogeneous.

Micro-acoustic properties of excised tissue should be measured to conclude the relation between 2D tissue strain and histology. For that purpose, we have already developed a quantitative acoustic microscope system that can measure speed of sound of the tissue components and we are planning to integrate the data obtained with quantitative IVUS and quantitative acoustic microscopy [5–7].

Detection of a vulnerable plaque by IVUS is important because plaque stabilization by pharmacological or genetic treatments may be available in near future. Today, if we detect a vulnerable plaque at IVUS study, the strategy for treatment is limited to coronary intervention. But distal protection devices are available to prevent slow flow or no-reflow phenomena caused by scattering of pre-existed thrombus and chemical mediator at the vulnerable plaque induced by coronary intervention.

5. Conclusions

In the present study, ultrasonic properties of atherosclerotic specimens excised by directional coronary atherectomy (DCA) are observed *in vivo* by IVUS tissue velocity imaging and are measured *in vitro* by optical microscopy. Two-dimensional tissue velocity and strain imaging showed different patterns in a stable plaque with collagen fibrosis or in a vulnerable plaque with various tissue components. Detecting a vulnerable plaque is important for decision of treatment strategy, at the present time, use of distal protection devices to prevent slow flow or no-reflow phenomena.

Acknowledgements

This study was supported by Grants-in-Aid for Scientific Research (Scientific Research (B) 13557059, 15300178) from the Japan Society for the Promotion of Science and Health and Labor Sciences Research Grants from the Ministry of Health, Labor and Welfare for the Research on Advanced Medical Technology (H17-Nano-001).

References

[1] C.L. de Korte, E.I. Cespedes, A.F. van der Steen, C.T. Lancee, Intravascular elasticity imaging using ultrasound: feasibility studies in phantoms, Ultrasound Med. Biol. 23 (1997) 735–746.

[2] C.L. de Korte, G. Pasterkamp, A.F. van der Steen, H.A. Woutman, N. Bom, Characterization of plaque components with intravascular ultrasound elastography in human femoral and coronary arteries in vitro, Circulation 102 (2000) 617–623.

[3] C.L. de Korte, M.J. Sierevogel, F. Mastik, C. Strijder, J.A. Schaar, E. Velema, G. Pasterkamp, P.W. Serruys, A.F. van der Steen, Identification of atherosclerotic plaque components with intravascular ultrasound elastography in vivo: a Yucatan pig study, Circulation 105 (2002) 1627–1630.

[4] J. Ophir, I. Cespedes, H. Ponnekanti, Y. Yazdi, X. Li, Elastography: a quantitative method for imaging the elasticity of biological tissues, Ultrason. Imaging 13 (1991) 111–134.

[5] Y. Saijo, H. Sasaki, H. Okawai, S. Nitta, M. Tanaka, Acoustic properties of atherosclerosis of human aorta obtained with high-frequency ultrasound, Ultrasound Med. Biol. 24 (1998) 1061–1064.

[6] Y. Saijo, H. Sasaki, S. Nitta, M. Tanaka, Visualization of human umbilical vein endothelial cells by acoustic microscopy, Ultrasonics 38 (2000) 396–399.

[7] Y. Saijo, C.S. Jorgensen, E. Falk, Ultrasonic tissue characterization of collagen in lipid-rich plaques in apoE-deficient mice, Atherosclerosis 158 (2001) 289–295.

Tohoku J. Exp. Med., 2006, **209**, 15-21

Impact of Type A Behavior on Brachial-Ankle Pulse Wave Velocity in Japanese

HONGJIAN LIU, YOSHIFUMI SAIJO, XIUMIN ZHANG,[1] YASUYUKI SHIRAISHI, YUN LUO,[2] MITSUYA MARUYAMA,[3] MASARU HIGA,[2] KAZUMITSU SEKINE and TOMOYUKI YAMBE

Department of Medical Engineering and Cardiology, Institute of Development, Aging and Cancer, Tohoku University, Sendai, Japan,
[1] Department of Medicine and Science in Sports and Exercise, Tohoku University Graduate School of Medicine, Sendai, Japan,
[2] Biomedical Engineering Research Organization, Tohoku University, Sendai, Japan, and
[3] Division of Medical Engineering and Clinical Investigation, Institute of Development, Aging and Cancer, Tohoku University, Sendai, Japan

LIU, H., SAIJO, Y., ZHANG, X., SHIRAISHI, Y., LUO, Y., MARUYAMA, M., HIGA, M., SEKINE, K. and YAMBE, T. *Impact of Type A Behavior on Brachial-Ankle Pulse Wave Velocity in Japanese.* Tohoku J. Exp. Med., 2006, **209**(1), 15-21 —— Pulse wave velocity (PWV) is the velocity of a pulse wave traveling a given distance between 2 sites in the arterial system, and is a well-known indicator of arteriosclerosis. Brachial-ankle PWV (baPWV) is a parameter more simple to obtain, compared with the conventional PWV, and is an easy and effective means of evaluating arteriosclerosis. BaPWV can be obtained by only wrapping the four extremities with blood pressure cuffs, and it can be easily used to screen a large number of subjects. Type A behavior has been confirmed as an independent risk factor for the development of coronary heart disease. To examine the relationship between Type A behavior and arteriosclerosis, 307 normal Japanese subjects were classified into either a Type A group (n = 90) or a non-Type A group (n = 217) by using Maeda's Type A Scale. BaPWV was evaluated using a PWV diagnosis device. The baPWV in the Type A group was significantly higher than that obtained in the non-Type A group. The baPWV showed a positive correlation with age both in the Type A group and in the non-Type A group; however, the straight-line regression slope of baPWV versus age in the Type A group was significantly larger than that in the non-Type A group. Therefore, our results suggest that arteriosclerosis might be promoted earlier in subjects expressing the Type A behavior pattern. Type A behavior pattern is confirmed as a risk factor for arteriosclerosis, and may increase the risk of the cardiovascular disease related to arteriosclerosis. ——— Type A behavior; Brachial-ankle pulse wave velocity; arteriosclerosis

Received December 14, 2005; revision accepted for publication March 6, 2006.
Correspondence: Hongjian Liu, Ph.D., Department of Medical Engineering and Cardiology, Institute of Development, Aging and Cancer, Tohoku University, 4-1 Seiryomachi, Aoba-ku, Sendai 980-8575, Japan.
e-mail: hongjianliu63@yahoo.co.jp

Type A behavior was first described by Friedman and Rosenman in the late 1950s, and it has since drawn considerable attention as a possible coronary risk factor. This behavior pattern includes impatience, aggressiveness, a sense of time urgency, an intense achievement drive, and a desire for recognition and advancement. In the Western Collaborative Group Study, the Type A behavior pattern was shown to be predictive of the incidence of coronary heart disease independently of the traditional risk factors such as smoking, hyperlipidemia, and hypertension (Buller et al. 1998; Yoshimasu 2001). Type A behavior may enhance the rate of development of coronary arteriosclerosis, and the presence and severity of coronary arteriosclerosis as determined by angiography have been investigated in relation to the presence and severity of Type A behavior (Sparagon et al. 2001). Type A behavior assessed by a questionnaire modified to Japanese characteristics and job strain has been linked to angiographically determined coronary arteriosclerosis (Yoshimasu et al. 2000; Gallacher et al. 2003).

Pulse wave velocity (PWV) is a well known indicator of arteriosclerosis. Many reports have described the relationship between PWV and the development of arteriosclerotic disease. Recent studies have demonstrated that PWV is not only a risk marker of cardiovascular disease, but is also a prognostic predictor (Altun et al. 2004; Fujiwara et al. 2004; Tomiyama et al. 2004, 2005; Woodside et al. 2004).

PWV is the velocity of a pulse wave traveling a given distance between 2 sites in the arterial system. Recently, a new, simple device to measure brachial-ankle pulse wave velocity (baPWV) has been developed using pressure cuffs wrapped around the brachium and ankle. BaPWV has potential as a new marker of cardiovascular risk over conventional markers, as it is easy to obtain and serves as an indicator of either arteriosclerotic cardiovascular risk or severity of arteriosclerotic vascular damage. Thus it can be useful in screening the general population (Yamashina et al. 2003; Yokoyama et al. 2003; Ogawa et al. 2005).

Therefore, we hypothesized that if Type A behavior could be a risk factor of arteriosclerosis, subjects expressing the Type A behavior pattern might show a higher baPWV. The aim of this study was to compare differences of baPWV between subjects showing Type A behavior and those not showing Type A behavior.

Materials and Methods

Subjects

Three hundreds and seven normal Japanese subjects participated in this study. The data were collected at Tohoku University, Sendai, Japan. The exclusion criteria were the following: hypertension (defined as systolic blood pressure [SBP] ≧ 140 mmHg, diastolic blood pressure [DBP] ≧ 90 mmHg, or drug treatment for hypertension), endocrine disease, significant renal or hepatic disease, coronary artery disease, arrhythmias, cerebrovascular disease, or use of medication for diabetes mellitus or hyperlipidemia. Written informed consent was obtained from all participants, and the study protocol was approved by the Ethics Committee of Tohoku University, Graduate School of Medicine and School of Medicine, Japan.

Measurement of the Type A behavior pattern

Type A behavior was assessed by an abbreviated set of 12 questions developed by Maeda (1991). This assessment is considered to be very practical for epidemiological investigations because of its convenience. Each question is listed in Table 1. The subjects were asked to answer all of the questions. Each question allowed three responses. Two, 1, and 0 points were assigned, respectively, to responses of "always", "occasionally", and "hardly" for questionnaire items 1, 2, 3, 4, 7, 8, 10, 11, and 12, and the points were doubled for questionnaire items 5, 6, and 9. A total score of 17 or greater was defined as Type A.

Measurement of baPWV

The subjects were examined while resting in the supine position. After at least a 5-minute bed rest, baPWV was recorded using an automated device (VaSeraVS-1000, Fukuda Denshi, Tokyo) (Liu et al. 2005; Watanabe et al. 2005). This device simultaneously records baPWV, blood pressure (BP), electrocardiogram, and heart sounds. Electrocardiogram electrodes were placed on both wrists, and a heart sound microphone was placed on the left sternal border. Cuffs to measure baPWV were wrapped around both upper arms and ankles, and connected to a plethysmographic sensor that

TABLE 1. *Maeda's questionnaire for Type A behavior pattern*

Questions	Always	Occasionally	Hardly
1. Do you have a busy daily life?			
2. Do you feel being pressed for time in your daily life?			
3. Do you easily become enthusiastic over your job or other things?			
4. When you are absorbed in your job, do you find it difficult to change your mind?			
5. Are you a perfectionist?			
6. Do you have confidence in yourself?			
7. Do you easily feel tense?			
8. Do you easily feel irritated or angry?			
9. Are you punctual with everything?			
10. Are you unyielding?			
11. Do you have an intense temper?			
12. Do you easily become competitive about job or other things?			

Each question had three responses. Points 2, 1, and 0 were given to the answers of "always", "occasionally", and "hardly" for 1, 2, 3, 4, 7, 8, 10, 11 and 12 nine questions, and the points were doubled for 5, 6 and 9 three questions. A total score of 17 or greater was defined as type A.

determines volume pulse form. Volume waveforms were stored for a sampling time of 10 s with automatic gain analysis and quality adjustment. This instrument simultaneously records the baPWV on the left and right sides. The highest baPWV on both sides was determined, and subsequent statistical analyses were performed using these values (Liu et al. 2005; Tomiyama et al. 2005).

Statistical analysis

Data are expressed as mean ± S.D. All statistical analyses were performed using StatView-5 software (SAS Institute Inc., Cary, NC, USA). Student's *t*-test was used to examine statistical difference of baPWV, BMI or SBP between subjects with Type A behavior and subjects without Type A behavior. Multiple linear regression analysis was performed to evaluate the association between baPWV and age, BMI, SBP, DBP, and Type A Scale in the subjects. Pearson's correlation coefficient analysis was used to assess the relation between baPWV and SBP in subjects with Type A behavior and subjects without Type A behavior and the relation between PWV and Type A Scale in 307 subjects. Partial correlation coefficient analysis was used to describe the correlation between baPWV and age using SBP as covariate. $p < 0.05$ was regarded as statistically significant.

RESULTS

Comparison of baPWV, BMI, and SBP between the Type A group and the non-Type A group

The subjects' characteristics are summarized in Table 2. Three hundreds and seven normal Japanese subjects were classified into either the Type A group ($n = 90$) or the non-Type A group ($n = 217$). BaPWV in the Type A group was significantly higher than that in non-Type A group. SBP and BMI were also significantly higher in the Type A group than those in the non-Type A group.

TABLE 2. *Characteristics of subjects*

Variables	Type A group	Non-Type A group
n	90	217
Age (years)	34.29 ± 16.54	33.92 ± 14.94
BMI (kg/m^2)	21.96 ± 2.94	21.24 ± 2.49*
BaPWV (m/sec)	11.88 ± 2.35	10.96 ± 1.25*
SBP (mmHg)	124.94 ± 8.24	122.27 ± 9.14*

Data represent mean ± S.D.
* $p < 0.05$ (Student's *t*-test).

Correlation of baPWV with age and SBP in the Type A group and in the non-Type A group

Table 3 shows the results of multiple regression analysis including baPWV and age, BMI, SBP, DBP, or Type A Scale. Age, SBP, and Type A Scale were significantly associated with baPWV, whereas BMI and DBP showed no significant association.

TABLE 3. *Multiple regression analysis of the factors associated with baPWV*

Variables	β	p value
Age	0.57	0.001
BMI	0.01	0.895
SBP	0.14	0.012
DBP	0.08	0.102
Type A Scale	0.29	0.001

After adjusting for SBP, baPWV showed a significant positive partial correlation with age both in the Type A group ($r = 0.72, p < 0.05$) (Fig. 1A) and in the non-Type A group ($r = 0.54, p < 0.05$) (Fig. 1B). Comparisons between straight-line regression slopes were made using an analysis of covariance. The slope of baPWV vs age in the Type A group ($Y = 7.946 + 0.102X$) was significantly larger than that in the non-Type A group ($Y = 10.251 + 0.044X$) ($F = 45.38, p < 0.001$).

BaPWV showed a significant positive correlation with SBP both in the Type A group ($r = 0.41$, $p < 0.05$) (Fig. 2A) and in the non-Type A group ($r = 0.31$, $p < 0.05$) (Fig. 2B). The slope of baPWV vs SBP in the Type A group ($Y = -2.831 + 0.118X$) was significantly larger than that in the non-Type A group ($Y = 5.816 + 0.042X$) ($F = 10.99, p < 0.001$).

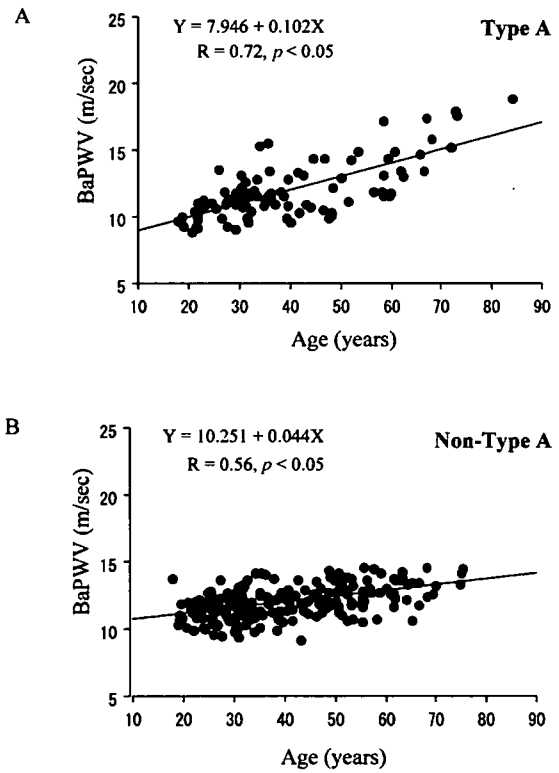

Fig. 1. Relations between baPWV and age adjusted for SBP in Type A group (A) and non-Type A group (B).

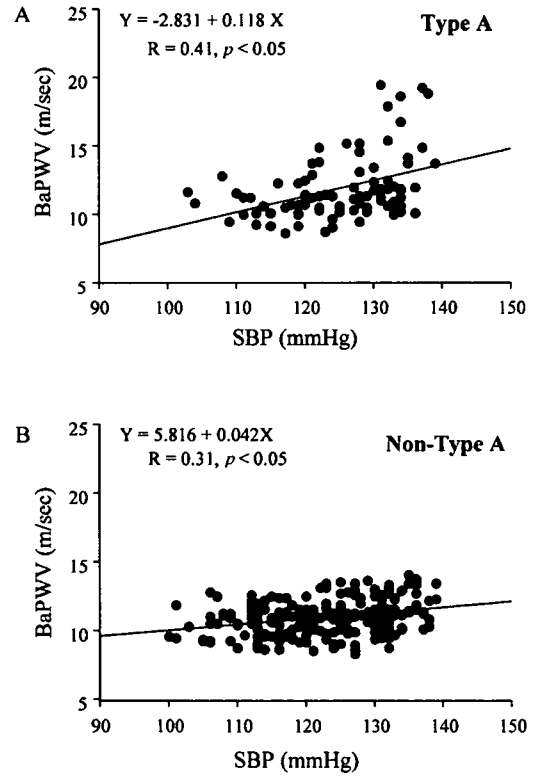

Fig. 2. Relations between baPWV and SBP in the Type A group (A) and in the non-Type A group (B).

Correlation of baPWV and SBP with the Type A Scale in 307 subjects

BaPWV showed a significant positive correlation with the Type A Scale in 307 subjects (r = 0.34, $p < 0.05$) (Fig. 3A). However, SBP showed no significant correlation with the Type A Scale (Fig. 3B).

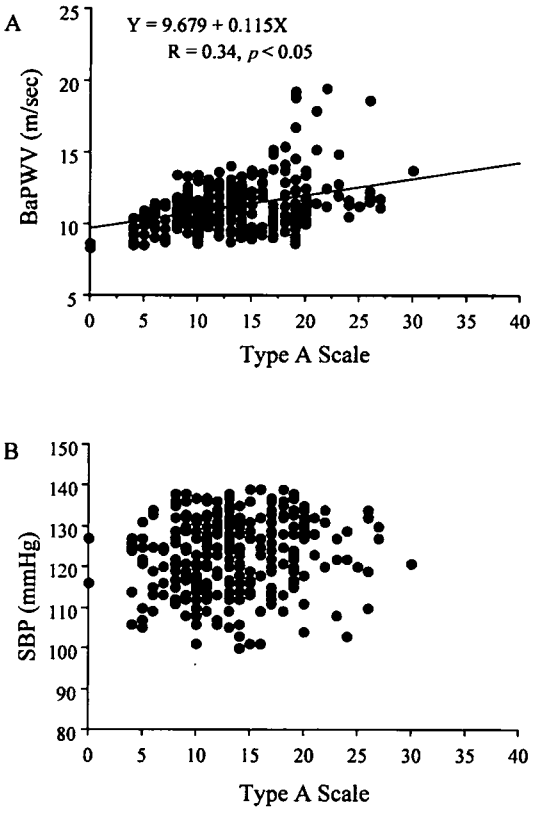

Fig. 3. Relations between baPWV and Type A Scale in 307 subjects (A) and Relations between SBP and Type A Scale in 307 subjects (B).

Discussion

In the present study, we compared the baPWV of subjects with Type A behavior and those without Type A behavior for the first time. Our major finding is that the baPWV of the Type A group had higher values than those of the non-Type A group. Therefore, our results suggest that subjects expressing the Type A behavior pattern have a higher risk for arteriosclerotic diseases than do subjects showing a non-Type A behavior pattern.

Arterial stiffness is a cause of premature return of reflected waves in late systole, increasing central pulse pressure and the load on the ventricle, reducing ejection fraction, and increasing myocardial oxygen demand (Laurent et al. 2001). The principal outcomes of these changes are left ventricular hypertrophy, aggravation of coronary ischemia, and increased fatigue of arterial wall tissues (Shoji et al. 2001; Blacher et al. 2003). Higher systolic blood pressure and pulse pressure, lower diastolic blood pressure, and left ventricular hypertrophy have been identified as independent factors of cardiovascular morbidity. Arterial stiffness is correlated with atherosclerosis, probably through the effects of cyclic stress on arterial wall thickening (Laurent et al. 2001).

The synergistic effect of hypertension and arteriosclerosis may appear as a higher PWV value. The degree of PWV elevation may correspond to the degree of arteriosclerotic change: a very high PWV may indicate that the arteriosclerotic process is already well established (Ogawa et al. 2003; Yokoyama et al. 2003). Thus, an increased PWV was associated with arteriosclerotic risk factors (Altun et al. 2004; Fujiwara et al. 2004; Tomiyama et al. 2004).

We also examined the correlation between baPWV and age. BaPWV showed a significantly positive correlation with age in subjects both with Type A behavior and in subjects without Type A behavior. The significant positive correlation found between baPWV and age showed that arteries become less elastic with age, and arterial stiffening was observed with increasing age (Oren et al. 2003). Aging induces structural and functional abnormalities such as arterial wall hypertrophy and degeneration or disorganization of the medial layer. These changes increase PWV because of increased arterial stiffness (Tomiyama et al. 2004, 2005).

Moreover, we found that the straight-line regression slope of baPWV vs age was significantly larger in subjects with Type A behavior than in subjects without Type A behavior. These results suggest that the increase of baPWV with age occurred earlier, the development of arterio-

sclerosis was faster, and an overall higher cardiovascular risk was shown in subjects expressing Type A behavior than in subjects not expressing Type A behavior. This trend may be associated with the effects on psychosocial variables of the Type A behavior pattern. A series of recent findings support adverse psychosocial effects relevant to arteriosclerosis under conditions of mental stress. Psychological variables may also impact the course of coronary disease through behavioral mechanisms (Rutledge et al. 2001).

Type A men, irrespective of coronary status, showed larger systolic and diastolic blood pressure response to both mental and physical stress than did Type B men (Sundin et al. 1995). Type A behavior may produce mental overload and stress, while coronary-prone exhaustion is characterized by inappropriate coping with environmental stress and giving up when confronted with life distress. Type A behavior is seen as personality traits, but it may also be a set of reactions to environmental stress and thus easily influenced by life events and working stress (Keltikangas-Jarvinen et al. 1996). Recently, it was reported that there exists a certain relationship between psychological factors and the extent of atherosclerosis measured by coronary angiography (Whiteman et al. 2000). There are few studies investigating the psychosocial factors related to these measures of arteriosclerotic disease processes. Psychosocial factors have been shown to contribute significantly to the development and clinical manifestations of coronary artery disease (CAD) (Whiteman et al. 2000). Type A behavior pattern is predictive of increased risk of coronary arteriosclerosis and might contribute to premature coronary arteriosclerosis and increased risk for CAD (Donker 2000; Yoshimasu et al. 2000, 2001; Sparagon et al. 2001).

Heart rate, lipid profiles and plasma glucose also influence PWV. However, these parameters were not examined in this study. It might be of interest to examine whether Type A behavior influences them.

In summary, the baPWV in the Type A group was significantly higher than that observed in the non-Type A group. The baPWV showed a positive correlation with age both in the Type A and the non-Type A groups. Moreover, the increasing trend of baPWV against age seen in the Type A group had a larger value than that of non-Type A group. Our results suggest that arteriosclerosis might be promoted earlier in subjects showing the Type A behavior pattern. Type A behavior pattern is confirmed as a risk factor for arteriosclerosis, and may promote to increase the risk of the cardiovascular disease related to arteriosclerosis. These findings may be associated with the differences in their psychosocial factors.

Acknowledgments

This work was partly supported by a Grant-in-aid for Scientific Research (11480253), a Research Grant for Cardiovascular Diseases from the Ministry of Health and Welfare and Program for Promotion of Fundamental Studies in Health Science of Organizing for Drug ADR Relief, R&D Promotion and Product Review of Japan, and Health and Labour Sciences Research Grants for Research on Advanced Medical Technology.

References

Altun, A., Erdogan, O. & Yildiz, M. (2004) Acute effect of DDD versus VVI pacing on arterial distensibility. *Cardiology*, **102**, 89-92.

Blacher, J., Safar, M.E., Guerin, A.P., Pannier, B., Marchais, S.J. & London, G.M. (2003) Aortic pulse wave velocity index and mortality in end-stage renal disease. *Kidney Int.*, **63**, 1852-1860.

Buller, J.C., Kritz-Silverstein, D., Barrett-Connor, E. & Wingard, D. (1998) Type A behavior pattern, heart disease risk factors, and estrogen replacement therapy in postmenopausal women: the Rancho Bernardo Study. *J. Womens Health*, **7**, 49-56.

Donker, F.J. (2000) Cardiac rehabilitation: a review of current developments. *Clin. Psychol. Rev.*, **20**, 923-943.

Fujiwara, T., Saitoh, S., Takagi, S., Ohnishi, H., Ohata, J., Takeuchi, H., Isobe, T., Chiba, Y., Katoh, N., Akasaka, H. & Shimamoto, K. (2004) Prevalence of asymptomatic arteriosclerosis obliterans and its relationship with risk factors in inhabitants of rural communities in Japan: Tanno-Sobetsu study. *Atherosclerosis*, **177**, 83-88.

Gallacher, J.E., Sweetnam, P.M., Yarnell, J.W., Elwood, P.C. & Stansfeld, S.A. (2003) Is type A behavior really a trigger for coronary heart disease events? *Psychosom. Med.*, **65**, 339-346.

Keltikangas-Jarvinen, L., Raikkonen, K., Hautanen, A. & Adlercreutz, H. (1996) Vital exhaustion, anger expression, and pituitary and adrenocortical hormones. Implications for the insulin resistance syndrome. *Arterioscler Thromb Vasc. Biol.*, **16**, 275-280.

Laurent, S., Boutouyrie, P., Asmar, R., Gautier, I., Laloux, B., Guize, L., Ducimetiere, P. & Benetos, A. (2001) Aortic stiffness is an independent predictor of all-cause and cardiovascular mortality in hypertensive patients. *Hyperten-*

sion, **37**, 1236-1241.

Liu, H., Yambe, T., Zhang, X., Saijo, Y., Shiraishi, Y., Sekine, K., Maruyama, M., Kovalev, Y.A., Milyagina, I.A., Milyagin, V.A. & Nitta, S. (2005) Comparison of brachial-ankle pulse wave velocity in Japanese and Russians. *Tohoku J. Exp. Med.*, **207**, 263-270.

Maeda, S. (1991) Application of a brief questionnaire for the behavior pattern survey. *Type A*, **2**, 33-40.

Ogawa, O., Onuma, T., Kubo, S., Mitsuhashi, N., Muramatsu, C. & Kawamori, R. (2003) Brachial-ankle pulse wave velocity and symptomatic cerebral infarction in patients with type 2 diabetes: a cross-sectional study. *Cardiovasc. Diabetol.*, **2**, 10.

Ogawa, O., Hayashi, C., Nakaniwa, T., Tanaka, Y. & Kawamori, R. (2005) Arterial stiffness is associated with diabetic retinopathy in type 2 diabetes. *Diabetes Res. Clin. Pract.*, **68**, 162-166.

Oren, A., Vos, L.E., Bos, W.J., Safar, M.E., Uiterwaal, C.S., Gorissen, W.H., Grobbee, D.E. & Bots, M.L. (2003) Gestational age and birth weight in relation to aortic stiffness in healthy young adults: two separate mechanisms? *Am. J. Hypertens.*, **16**, 76-79.

Rutledge, T., Reis, S.E., Olson, M., Owens, J., Kelsey, S.F., Pepine, C.J., Reichek, N., Rogers, W.J., Merz, C.N., Sopko, G., Cornell, C.E. & Matthews, K.A. (2001) Psychosocial variables are associated with atherosclerosis risk factors among women with chest pain: the WISE study. *Psychosom. Med.*, **63**, 282-288.

Shoji, T., Emoto, M., Shinohara, K., Kakiya, R., Tsujimoto, Y., Kishimoto, H., Ishimura, E., Tabata, T. & Nishizawa, Y. (2001) Diabetes mellitus, aortic stiffness, and cardiovascular mortality in end-stage renal disease. *J. Am. Soc. Nephrol.*, **12**, 2117-2124.

Sparagon, B., Friedman, M., Breall, W.S., Goodwin, M.L., Fleischmann, N. & Ghandour, G. (2001) Type A behavior and coronary atherosclerosis. *Atherosclerosis*, **156**, 145-149.

Sundin, O., Ohman, A., Palm, T. & Strom, G. (1995) Cardiovascular reactivity, Type A behavior, and coronary heart disease: comparisons between myocardial infarction patients and controls during laboratory-induced stress. *Psychophysiology*, **32**, 28-35.

Tomiyama, H., Arai, T., Koji, Y., Yambe, M., Hirayama, Y., Yamamoto, Y. & Yamashina, A. (2004) The relationship between high-sensitive C-reactive protein and pulse wave velocity in healthy Japanese men. *Atherosclerosis*, **174**, 373-377.

Tomiyama, H., Koji, Y., Yambe, M., Shiina, K., Motobe, K., Yamada, J., Shido, N., Tanaka, N., Chikamori, T. & Yamashina, A. (2005) Brachial - ankle pulse wave velocity is a simple and independent predictor of prognosis in patients with acute coronary syndrome. *Circ. J.*, **69**, 815-822.

Watanabe, I., Tani, S., Anazawa, T., Kushiro, T. & Kanmatsuse, K. (2005) Effect of pioglitazone on arteriosclerosis in comparison with that of glibenclamide. *Diabetes. Res. Clin. Pract.*, **68**, 104-110.

Whiteman, M.C., Deary, I.J. & Fowkes, F.G. (2000) Personality and social predictors of atherosclerotic progression: Edinburgh Artery Study. *Psychosom. Med.*, **62**, 703-714.

Woodside, J.V., Mcmahon, R., Gallagher, A.M., Cran, G.W., Boreham, C.A., Murray, L.J., Strain, J.J., Mcnulty, H., Robson, P.J., Brown, K.S., Whitehead, A.S., Savage, M. & Young, I.S. (2004) Total homocysteine is not a determinant of arterial pulse wave velocity in young healthy adults. *Atherosclerosis*, **177**, 337-344.

Yamashina, A., Tomiyama, H., Arai, T., Hirose, K., Koji, Y., Hirayama, Y., Yamamoto, Y. & Hori, S. (2003) Brachial-ankle pulse wave velocity as a marker of atherosclerotic vascular damage and cardiovascular risk. *Hypertens. Res.*, **26**, 615-622.

Yokoyama, H., Shoji, T., Kimoto, E., Shinohara, K., Tanaka, S., Koyama, H., Emoto, M. & Nishizawa, Y. (2003) Pulse wave velocity in lower-limb arteries among diabetic patients with peripheral arterial disease. *J. Atheroscler. Thromb.*, **10**, 253-258.

Yoshimasu, K., Liu, Y., Kodama, H., Sasazuki, S., Washio, M., Tanaka, K., Tokunaga, S., Kono, S., Arai, H., Koyanagi, S., Hiyamuta, K., Doi, Y., Kawano, T., Nakagaki, O., Takada, K., Nii, T., Shirai, K., Ideishi, M., Arakawa, K., Mohri, M. & Takeshita, A. (2000) Job strain, Type A behavior pattern, and the prevalence of coronary atherosclerosis in Japanese working men. *J. Psychosom. Res.*, **49**, 77-83.

Yoshimasu, K. (2001) Relation of type A behavior pattern and job-related psychosocial factors to nonfatal myocardial infarction: a case-control study of Japanese male workers and women. *Psychosom. Med.*, **63**, 797-804.

Multiple Parametric IVUS Imagings for Detection of Vulnerable Plaque

Yoshifumi Saijo, Esmeraldo dos Santos Filho, Tomoyuki Yambe
Department of Medical Engineering and Cardiology
Institute of Development, Aging and Cancer, Tohoku University
Sendai, Japan
saijo@idac.tohoku.ac.jp

Akira Tanaka
Faculty of Symbiotic Systems Science, Fukushima University
Fukushima, Japan

Takahiro Iwamoto, Shuo Li, Makoto Yoshizawa
Graduate School of Engineering, Tohoku University
Sendai, Japan

Abstract— **Detection of vulnerable plaque is important for decision making of the interventional strategy and for understanding pathophysiology of acute coronary syndrome. We have been developing some quantitative evaluation methods of IVUS imaging mainly by analyzing original RF signal. Recently, we have been interested in the region "behind the plaque" because inflammation or neovascularization of adventitia may contribute to the development of atherosclerosis. Clinically, so called "attenuation plaque" is a typical feature of vulnerable plaque. In the present study, we will present multiple parametric IVUS imagings such as conventional IVUS, integrated backscatter (IB), Virtual Histology™ (VH), 1D/2D strain imaging, self-organizing map (SOM), automatic calcium detection and attenuation imaging for visualization attenuation plaques.**

The evaluation of vulnerable plaque by multiple parametric IVUS analyses provides important information for assessment of acute coronary syndrome.

Keywords-intravascular ultrasound (IVUS); parametric imaging; attenuation plaque, vulnerable plaque

I. INTRODUCTION

Intravascular ultrasound (IVUS) has been clinically applied since early 1990's and it has become an important clinical tool for investigation of coronary artery during percutaneous transluminal coronary intervention (PCI) therapies. IVUS is mainly used to measure the luminal and vascular areas and to confirm the full expansion of the coronary stent to the arterial wall. Besides the measurement of dimensions, IVUS also provides important information on tissue character of atherosclerosis.

Recently, many clinical and experimental studies show that the vulnerable plaque in coronary artery is the main cause of acute coronary syndrome. Classical pathological definition of vulnerable plaque is a thin fibrous cap fibroatheroma with infiltration of inflammatory cells. Thus, much attentions have been paid to intimal lesion. However, recent studies have shown that the inflammation or neovascularization in the adventitia are strongly associated with development of vulnerable plaque.

Search for vulnerable plaque in clinical settings becomes very important. The biomarkers such as high sensitivity CRP (C-reactive protein), IL-6 (Interleukin-6) indicating inflammation are used as screening of vulnerable plaque. As IVUS visualizes coronary artery directly, it should provide important information of vulnerable plaque. Clinically, so called "attenuation plaque" is a typical feature of vulnerable plaque. Attenuation plaque is a low echo region without surface high scattering echo and that feature is different from acoustic shadow. Sometimes, it causes "no-reflow" or "slow flow" following PCI. The cause of slow flow may be release of inflamattory cytokines or thrombus by artificial plaque disruption by PCI.

From the point of pathology and clinical experience, we believe that the region "behind the plaque" should be the target of searching vulnerable plaque and we have developed serial parametric IVUS imagings. In the present study, we will present multiple parametric IVUS imagings such as conventional IVUS, integrated backscatter (IB), Virtual HistologyTM (VH), 1D/2D strain imaging, self-organizing map (SOM), automatic calcium detection and attenuation imaging for visualization attenuation plaques.

II. METHODS

A. Recording of RF signal

Commercial available IVUS systems (Galaxy2 or Clear View Ultra, Boston Scientific, USA) were equipped. The central frequency of the IVUS probe (Atlantis SR Pro, Boston Scientific, USA) was 40 MHz and the pulse repetition rate was

7680 Hz. A single frame of the IVUS system consisted of 256 lines so that 7680 pulses made 30 frames per second (f/s). An analogue to digital (A/D) converter board (CompuScope 8500, Gage, USA or DP310, Acqiris, Switzerland) was connected to the RF (radio-frequency signal) output of the IVUS apparatus. The sampling rate was 500 megasamples per second (MSa/s), the resolution was 8-bit and the on-board memory was 128 MB in the Gage A/D board. The sampling rate was 400 megasamples per second (MSa/s), the resolution was 12-bit and the on-board memory was 6 MB in the Acqiris A/D board. Intra-coronary pressure was measured by fluid-filled method using 6 French (2.0 mm) diameter guiding catheter which was inserted into coronary artery.

Biological signals such as electrocardiogram and intra-coronary pressure were simultaneously recorded using an A/D converter (PCI-6024E, National Instruments, USA) with the sampling rate of 100 kSa/s and the resolution of 12-bit. After the RF data were sent to a personal computer, 10 to 80 MHz components of the original RF signal were extracted by using a software-based bandpass filtering method.

Ideally, one frame consisting of 256 lines of the rotational IVUS is equivalent to that of phased-array IVUS. However, a conventional rotating IVUS system uses frame trigger to adjust frame to frame rotational non-uniformity. This indicates the position of the 'n/256'th line is not guaranteed to be at the same position of the previous frame. Then the correlation coefficient between two consecutive matrixes was calculated in the rotational direction and the rotational dis-uniformity was corrected in rotational direction to obtain the maximum correlation coefficient.

B. *Parametric IVUS Imagings*

Serial parametric IVUS imagings are reconstructed from the obtained RF signal. Integrated backscatter (IB) image was produced from the absolute value of time-domain RF signal instead of classical frequency-domain power spectrum of RF signal described in the original IB definition because each power should show same value when the signal was digitized completely. The image of 1D or 2D tissue strain was described in the previous paper [1, 2]. Self-organizing map (SOM) is a neural network that reduces dimensions and display similarities. The shape of power spectra of 256 points of an RF signal was characterized by 18 parameters for SOM [3]. Automatic calcium detection was based on adaptive thresholdngs and high intensity echo with acoustic shadow is defeined as calcium. Virtual Histology™ is also a neural network classification based on power spectrum of RF signal [4]. Attenuation imaging is a preliminary imaging method. The assumption that the total power of transmitted ultrasound from IVUS probe is equal in all direction is the basis of attenuation imaging. The differences of the IB between adjunctive regions of interest on a single IVUS line were considered as uncorrected attenuation coefficient. Then the attenuation coefficient was calibrated as to equalize the total power.

III. RESULTS

A. *Integrated Backscatter*

Figure 1 is a conventional IVUS image reconstructed from RF signal. Figure 2 is the IB image with color of the same region. The resolution is compatible with the sensitivity in conventional IVUS image. The sensitivity is prior to the resolution in IB, however, the image quality seems no difference in this setting.

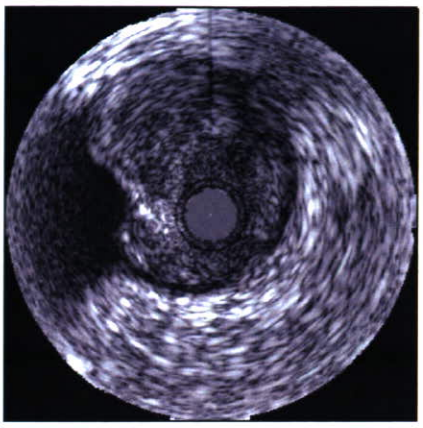

Figure 1. Example of a conventional IVUS image

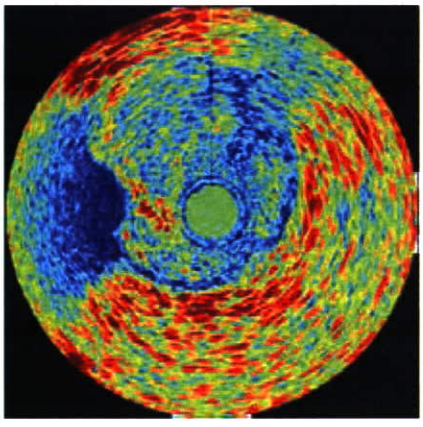

Figure 2. Example of an IB image of the same region of Figure 1

B. *1D Tissue Strain Image*

Figure 3 is 1D tissue strain image of the same region. Dark blue indicates the strain is low and the light blue indicates the strain is high. The region of 10 to 12 o'clock has a high strain that may indicate the soft contents such as lipid.

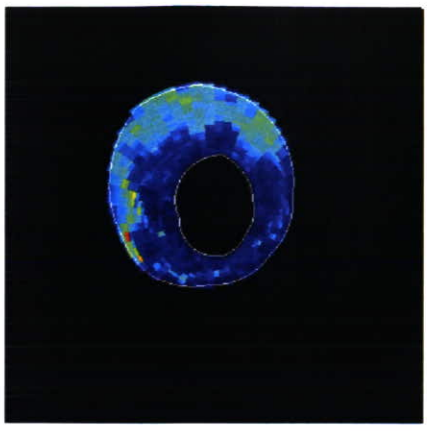

Figure 3. Example of an iD strain image of the same region of Figure 1

C. 2D Tissue Velocity and Strain Images

Figure 4 is 2D tissue velocity and Figure 5 is 2D tissue strain image.

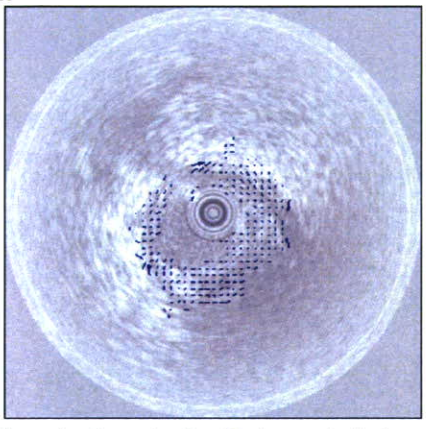

Figure 4. Example of an 2D tissue velocity image

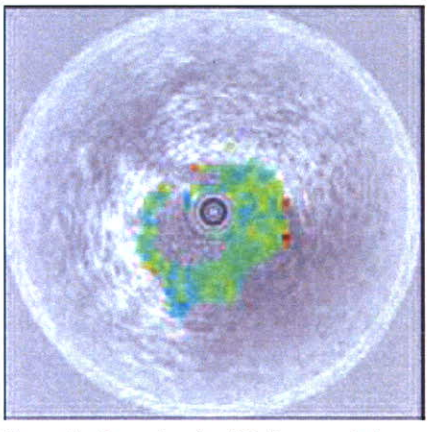

Figure 5. Example of an 2D tissue strain image

D. Virtual Histology™

Virtual HistologyTM classifies the coronary intima into four categories based on a neural network of the power spectra of RF signal. The four categories are fibrous, fibrofatty, calcium and necrotic core. Virmani insists on the necrotic core is the main feature of vulnerable plaque. There are still some discussions on the necrotic core among the clinical cardiologists. Figure 6 is VH image produced by us from the spectral analysis of the RF signal. Figure 7 is the VH image of the same region obtained by commercially available Volcano IVUS apparatus. In both images, outer region at 6 to 9 o'clock shows fibrofatty component while the intima of the same direction shows calcium.

Figure 6. VH image produced by our system.

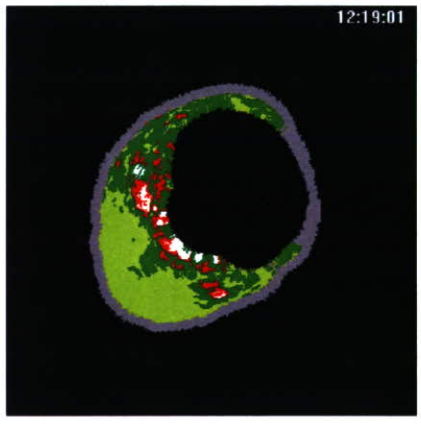

Figure 7. VH image obtained by Volcano IVUS apparatus.

E. Self-organizing Map (SOM)

Figure 8 is an example of SOM image of the same region in Figures 1, 2 and 3. Adventitial side is also classified in the SOM image.

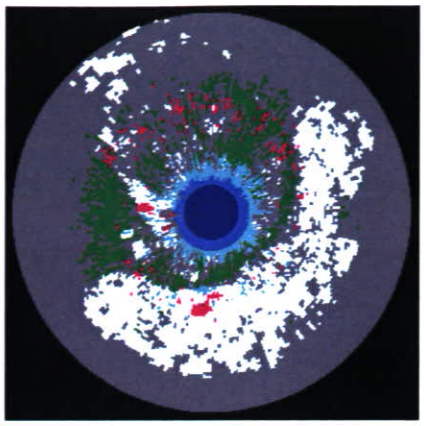

Figure 8. Example of a SOM image

F. Calcium Detection

Figure 9 is an IVUS image of calcification identified manually by three expert medical doctors. Figure 10 is the automatic detection of calcium.

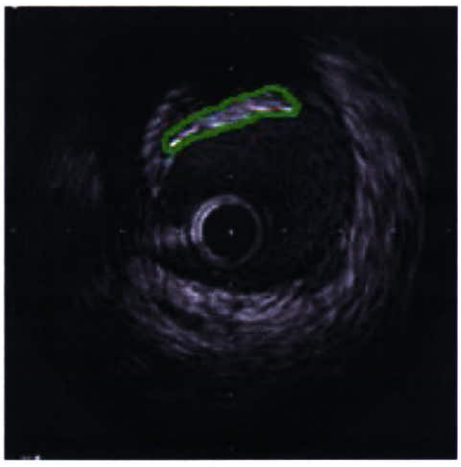

Figure 9. Manually defined calcium

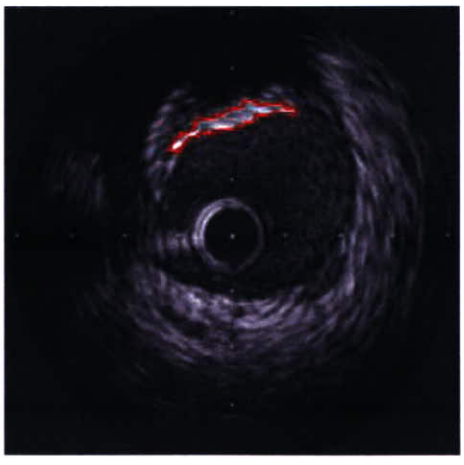

Figure 10. Automatic detection of calcium

G. Attenuation Imaging

The assumption that the total power of transmitted ultrFigure 11 is a conventional IVUS image and Figure 12 is the attenuation imaging of the same region. Guidewire shadow at 11 o'clock is compensated in attenuation imaging. The vein is clearly shown in the attenuation imaging while is is not obvious in the conventional IVUS imaging.

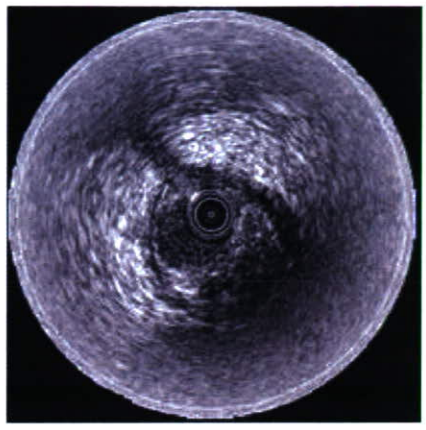

Figure 11. Conventional IVUS image

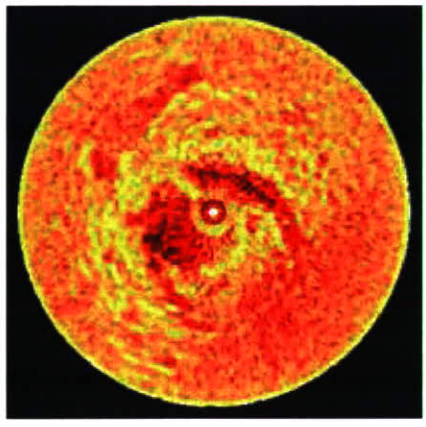

Figure 12. Attenuation imaging of the same region

IV. Conclusions

The evaluation of vulnerable plaque by multiple parametric IVUS analyses provides important information for assessment of acute coronary syndrome.

Acknowledgment

This study was supported by Grants-in-Aid for Scientific Research (Scientific Research (B) 13557059, 15300178) from the Japan Society for the Promotion of Science, Health and Labor Sciences Research Grants from the Ministry of Health, Labor and Welfare for the Research on Advanced Medical Technology (H17-Nano-001) and The Grant on Three Dimensional Organ Regeneration Program from New Energy and Industrial Technology Development Organization.

REFERENCES

[1] Saijo Y, Tanaka A, Owada N, Akino Y, Nitta S. Tissue velocity imaging of coronary artery by rotating-type intravascular ultrasound. *Ultrasonics*, Vol. 42, No. 1-9, 753-757, 2004.

[2] Saijo Y, Tanaka A, Iwamoto T, Dos Santos Filho E, Yoshizawa M, Hirosaka A, Kijima M, Akino Y, Hanadate Y, Yambe T. Intravascular two-dimensional tissue strain imaging. *Ultrasonics*. 2006 Jul 5; [Epub ahead of print]

[3] Iwamoto T, Tanaka A, Saijo Y, Yoshizawa M. Coronary plaque classification through intravascular ultrasound radiofrequency data analysis using self-organizing map. *Proc 2005 IEEE International Ultrasonics Symposium*, 2054-2057, 2005.

[4] Nair A, Kuban BD, Tuzcu EM, Schoenhagen P, Nissen SE, Vince DG. Coronary plaque classification with intravascular ultrasound radiofrequency data analysis. *Circulation*.Vol. 106, No. 17, 2200-6, 2002.